

1 **Spatially non-continuous relationships between biological invasion and** 2 **fragmentation of mangrove forests**

3 Zhen Zhang¹, Jing Li¹, Yi Li^{1,2*}, Wenwen Liu¹, Yuxin Chen¹, Yihui Zhang^{1,2}, Yangfan Li^{1,2}

4 1 Key Laboratory of Coastal and Wetland Ecosystems (Ministry of Education), College of the Environment and
5 Ecology, Xiamen University, Xiamen, 361102, China

6 2 Fujian Provincial Key Laboratory for Coastal Ecology and Environmental Studies, College of the Environment
7 and Ecology, Xiamen University, Xiamen, 361102, China

8 * Corresponding Author: yili@xmu.edu.cn

9 10 **Abstract**

11 Rapid and large-scale biological invasion results in widespread biodiversity loss and
12 degradation of essential ecosystem services, especially in mangrove forests. Recent evidence
13 suggests that the establishment and dispersal of invasive species may exacerbated in
14 fragmented landscape, but the influence of mangrove fragmentation on coastal biological
15 invasion at landscape scale remains largely unknown. Here, using the derived 10-m resolution
16 coastal wetland map in southeast coast of China, we examine the relationships between
17 fragmentation of mangrove forests and salt marsh invasion magnitude and quantify the
18 geographical variations of the relationships across a climatic gradient. Our results show that
19 mangrove forests with small size, large edge proportion, and regular boundary shape tend to
20 suffer more serious salt marsh invasions, indicating a positive correlation between mangrove
21 fragmentation and its invaded magnitude. In particular, such fragmentation-invasion
22 relationships in subtropics are shown to be more intensive than in tropic. Our findings provide
23 the first spatially explicit evidence of the relationships between mangrove fragmentation and
24 biological invasion on a landscape scale, and highlight an urgent need for conservation and
25 management actions to improve mangrove connectivity, which will increase resistance to
26 invasions, especially for small-size subtropical mangrove forests.

27 **Keywords:** mangrove management, invasive species, latitudinal gradient, coastal wetlands,
28 seascape ecology, remote sensing

29 **1. Introduction**

30 In exotic species-introduce hotspots such as the coastal area, biological invasion is
31 becoming a major driver of biodiversity decline and losses of ecological services in coastal
32 forests (Bellard et al., 2016; Slingsby et al., 2017). As the dominated woody wetland
33 community along tropical and subtropical coastlines, mangrove forests are particularly
34 sensitive to invasive species due to the narrow habitat niche within the intertidal environment
35 for species competition and intensive anthropogenic disturbances which limits their ability to
36 migrate landward (Bradley et al., 2012). While only covering a small portion of the Earth's
37 surface, mangrove forests provide a diversity of essential ecosystem services far beyond the
38 land area they occupy, such as coastal protection, carbon sequestration, erosion prevention, and
39 habitat for fisheries (Donato et al., 2011; Worthington et al., 2020). However, the supply of
40 these key ecosystem services has been threatening as mangroves are invaded by more than 50
41 plant species globally (Biswas et al., 2018). For example, woody mangroves invaded by
42 herbaceous salt marshes reduce their carbon storage and slow down rates of sediment accretion
43 in response to sea level rise (Kelleway et al., 2017). In addition to biological invasion,
44 expansion in aquaculture, logging and coastal reclamation has led to unprecedented
45 fragmentation of mangrove forests in recent few decades (Bryan-Brown et al., 2020; Richards
46 & Friess, 2016). Fragmentation of mangrove communities may raise exposure to exotic species
47 along forest edges (Dawson et al., 2015), further increasing their ecological sensitivity to
48 invasive species. In the light of such potential intersection, efforts to understand the impacts of
49 mangrove fragmentation on biological invasion have become critical for effective management
50 action.

51 Growing evidence suggests that landscape fragmentation would promote the establishment
52 of invasive species, and resident native species in fragment landscape are more likely to expose
53 to invader (Malavasi et al., 2014; Vilà & Ibáñez, 2011). For example, positive correlations have

54 been reported between landscape fragmentation and exotic species richness, as well as
55 abundance in both tropical rainforest and subtropical dry forest (Aguirre-Acosta et al., 2014;
56 Waddell et al., 2020). This fragmentation-invasion relationship can partly be interpreted as
57 transformation of biophysical environments near habitat fragment edges (Ordway & Asner,
58 2020). However, this was concluded in terrestrial ecosystems, illustrating our poor knowledge
59 on the relationships between coastal mangrove fragmentation and biological invasions. In
60 contrast to terrestrial forests, mangroves could be invaded by both aquatic and terrestrial
61 species (Biswas et al., 2018). Additionally, limited habitats in intertidal environments and
62 relatively smaller size of mangrove patches imply that fragmentation in mangrove patches may
63 have more complicated consequences contrast with terrestrial forests. As such, conclusion
64 derived in terrestrial forests could not be directly transformed to coastal mangrove forests. A
65 better understanding of fragmentation-invasion relationships in mangrove ecosystems is
66 required to warn potential invaded mangrove communities, and also to perform efficient
67 management strategies in the context of anthropogenic land-use change.

68 The establishment and spread of alien species are affected by both biotic factors and abiotic
69 conditions (Liu et al., 2018; van Kleunen et al., 2018), including species richness of native
70 communities (Beaury et al., 2020), competitive and consumptive interactions (Alofs & Jackson,
71 2014), resident herbivores (Zhang et al., 2018) and local temperature (Cornelissen et al., 2019).
72 Due to the spatial heterogeneity of these conditions, invasive ability of alien species and
73 resistant of native species to invasion may not spatially continuous across the landscape (Stotz
74 et al., 2016). As a result, invasion processes and outcomes may vary among different climate
75 zones such as tropic and subtropics. Understanding how this geographical variation affect
76 invasion pattern thus is fundamental to identify vulnerable areas where are particularly
77 sensitive to invasion, as well as developing conservation strategies in advance. However,
78 earlier studies on fragmentation-invasion relationships mostly conducted in site level, can be

79 sensitive to the local environmental conditions (Oehri et al., 2017), constrained by their poor
80 spatial coverage while ignoring the geographical variations of fragmentation-invasion
81 relationships. While some studies monitored the spatial distribution of invasive species in a
82 larger scale by using remote sensing approaches (Liu et al., 2018; Vaz et al., 2018), there is
83 still uncertainties about how the fragmentation-invasion relationship varies across a climatic
84 gradient.

85 Here, we adopt a biogeographic perspective to test whether the mangrove fragmentation has
86 impacts on the invasion magnitude of an invasive saltmarsh species (*Spartina alterniflora*)
87 along latitudinal gradient in Southeastern China, a region that has undergone widespread *S.*
88 *alterniflora* invasion over the last several decades (Meng et al., 2020). We characterize
89 mangrove fragmentation from three key aspects, including fragment size, edge, and shape,
90 which have been widely used in fragmentation researches (Haddad et al., 2015; Mendes et al.,
91 2016). The main purposes of this study are: (a) to test the latitudinal pattern in invasion
92 magnitude of *S. alterniflora* on mangrove forests, (b) to specify the impacts of mangrove
93 fragmentation on *S. alterniflora* invasion magnitude, and (c) to detect the geographic variations
94 in fragmentation-invasion relationship along climatic gradient.

95

96 **2. Materials and Methods**

97 **2.1. Study Area**

98 The Southeast coastal areas of China provide an ideal setting to examine the invaded
99 pattern of native wetland plants on a landscape scale as the area has suffered from a long-term
100 *S. alterniflora* invasion and is one of the most sensitive mangrove-marsh ecotones in the world
101 to changes in climatic conditions (Osland et al., 2016). *S. alterniflora* was introduced and
102 spread over a 19°-latitude region along the east coast of China since 1979 (Liu et al., 2016),
103 and dominated a large area of tidal flats in past two decades, occupying approximately 545.80

104 km² of coastal zone in 2015 (Liu et al., 2018). This study was conducted within the coastal
105 areas in the southeast of mainland China, which spans a latitudinal gradient extending from
106 tropical Leizhou Peninsula in the south (~20°34'N) to subtropical Zhejiang Province
107 (~28°25'N), covering the whole geographical range of mangrove-salt marsh ecotone in
108 mainland China (Chen et al., 2017).

109 **2.2. Characterizing mangrove fragmentation**

110 *2.2.1. Fragment size*

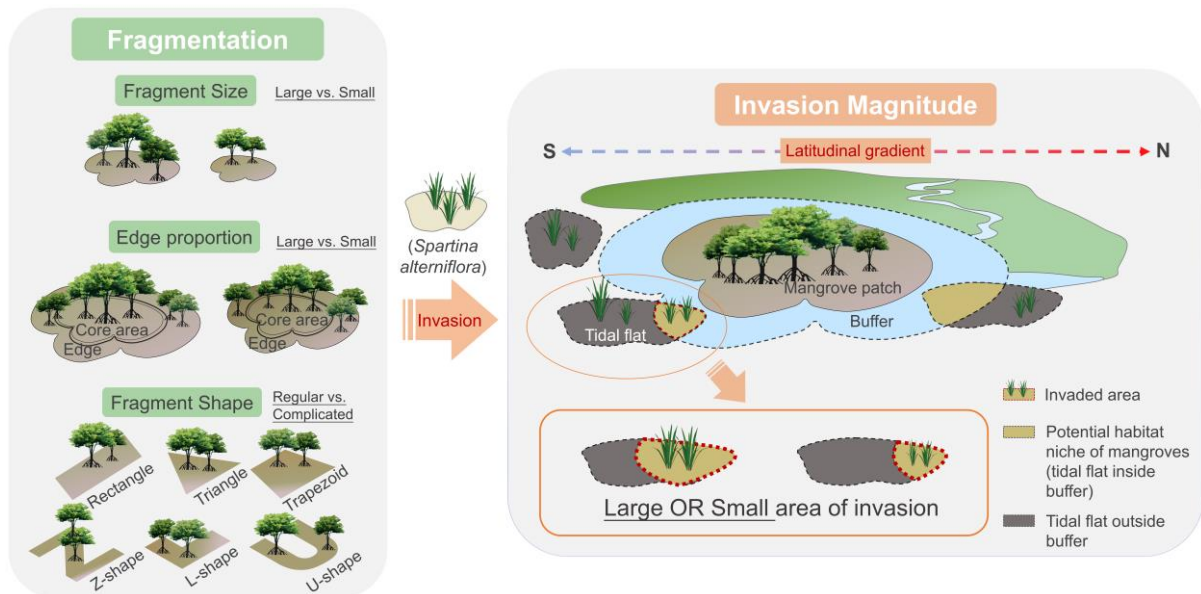
111 We mapped the distribution of mangroves and *S. alterniflora* in 2020 using all available
112 atmospherically corrected Sentinel-2 surface reflectance product on Google Earth Engine
113 platform (Gorelick et al., 2017). The derived coastal wetland dataset at 10-m resolution enables
114 a high-accuracy assessment of relationship between mangroves and *S. alterniflora* (88.7%
115 overall accuracy; see Supplementary Information for more details). Since the fragmentation
116 process is inevitably resulted from the reduction of the patch area, we used the mangrove
117 fragment size as a metric to measure fragmentation (Haddad et al., 2015). The size (unit: ha)
118 of each mangrove fragment was then calculated based on the derived wetland dataset using an
119 Albers conic equal-area projection.

120 *2.2.2. Edge proportion*

121 A mangrove fragment is composed of edge and core area (Fig. 1). Mangrove edge is
122 defined as any mangrove pixel adjacent to a non-mangrove pixel, and the mangrove core is the
123 remaining mangrove pixels (Chaplin-Kramer et al., 2015). The specific process of edge area
124 identification was carried out using a sum filter with a three by three window (8 neighbors) on
125 the binary mangrove/non-mangrove image, in which mangrove pixels were assigned with value
126 of 1 and the non-mangrove pixels with value of 0. Mangrove pixel was considered as a grid of
127 'core area' only if its value equals to 9 based on the spatial filter process; otherwise, it was
128 classified as 'edge area'. We calculated the edge proportion in each mangrove fragment (i.e.

129 the ratio of edge area to mangrove fragment area), and used it as a fragmentation metric to
130 explore the edge effect of mangrove fragments to *S. alterniflora* invasion.

131



132

133 **Fig. 1.** Conceptual diagram of seascape patterns of mangrove fragments and the *S. alterniflora* invasion magnitude.

134

135 2.2.3. Fragment shape

136 We proposed an information theory-based approach to identify the specific shape of grid-
137 cell mangrove fragments (Supplemental Fig. S2; see Supplementary Information for more
138 details). To group all fragments into certain shapes, we predefined six standard shapes as
139 rectangle, triangle, trapezoid, Z-shape, L-shape, and U-shape, since these shapes can
140 approximately describe most of our pixel-based mangrove fragments according to visual
141 inspection. The first three shapes were classified as regular shapes and the others as
142 complicated shapes for extracting conclusive information (Supplemental Fig. S3). The reason
143 we use specific shapes rather than shape complexity to reflect the shape effect is that specific
144 shapes are practical in guiding mangrove restoration.

145 For each mangrove fragment, the distances of centroid to fragment boundary measured
146 from all directions were plotted as a continuous signal (Supplemental Fig. S2). Jensen-Shannon

147 (JS) divergence (Lin, 1991), an information theory-based metric to assess the similarity
148 between two signals, was then used to compare the signal of each mangrove fragment with
149 signal of standard shapes. By comparing the identified signal of each fragment and that of
150 standard shape, we assigned every mangrove fragment to certain shape group, which can be
151 further grouped to regular and complicated shapes. All spatial related processes were conducted
152 in Python 2.7, and more details about our information theory-based approach are provided in
153 Supplementary Information.

154 **2.3. Quantifying *S. alterniflora* invasion magnitude**

155 *S. alterniflora* tend to occur on the bare tidal flats close to the margins of mangrove forest
156 or within the canopy gaps of sparse mangroves (Chen et al., 2016). Our earlier experiment
157 (Zhang et al., 2012) demonstrated *S. alterniflora* transplanted into the understory of dense
158 mangrove stands died in a period of time, implying that the invasion of *S. alterniflora* did not
159 directly occupy areas of mangroves, but the surrounding bare tidal flats of mangrove forests to
160 limit the mangrove propagation. Thus, the *S. alterniflora* invasion magnitude was defined as
161 the proportion of surrounding tidal flats occupied by *S. alterniflora* to the total bare tidal flats
162 around mangrove forests (Fig. 1).

163 Under this circumstance, we firstly determined which bare tidal flats have the potential to
164 support mangrove propagation based on the historic expansion distance of mangrove forests.
165 Specifically, we calculated the historical expansion distance of mangroves during the past two
166 decades using the multi-temporal global mangrove maps from the Global Mangrove Watch
167 dataset (Bunting et al., 2018). Considering the capability of mangrove propagation would be
168 spatially heterogeneous, we calculated the distance per 1° latitudinal band, and used it as the
169 radius to create buffer area for related mangrove fragments. Bare tidal flats in created buffer
170 zone were identified as potential habitat for mangrove propagation. Subsequently, based on the
171 global tidal flat dataset (Murray et al., 2019) and our *S. alterniflora* map, we recorded the tidal

172 flats area and *S. alterniflora* area within the surrounding potential habitat separately, and
173 calculated the ratio of the *S. alterniflora* area to the area of tidal flats as the measure of invasion
174 magnitude. The calculated invasion magnitude was bounded between value 0 and 100%, and a
175 higher number means that more of the tidal flats where mangroves have the potential to
176 propagate has been invaded by *S. alterniflora*.

177 **2.4. Statistical analysis**

178 *2.4.1. Detecting latitudinal patterns*

179 To analyze the detailed latitudinal variations of invaded magnitude and fragmentation of
180 mangrove communities, we averaged these metrics in each of the 0.1° latitudinal bands. We
181 then used ordinary least squares regression models to estimate the biogeographical trend in
182 invasion magnitude and fragmentation metrics along latitudinal gradient, and the significance
183 of the models were assessed. Considering the shape index of mangrove fragments is a
184 qualitative variable, and all mangrove fragments were divided into two groups (regular and
185 complicated shapes), we calculated the proportion of mangrove fragments in both groups per
186 0.1° latitudinal band, and used it to represent latitudinal variation in fragment shapes.
187 Additionally, to examine the difference of invasion magnitude in different climate zones, we
188 compared *S. alterniflora* invasion magnitude between the tropical and subtropical mangrove
189 fragments by using dependent *t*-test at fragment scale.

190 *2.4.2. Effects of fragment size on invasion magnitude*

191 To specify the effect of mangrove fragment size on *S. alterniflora* invasion, we aggregated
192 mangrove fragments with similar sizes into same group by using *K*-means algorithm and
193 obtained 83 and 60 fragment groups for tropical and subtropical regions, respectively.
194 Aggregating mangrove fragments of similar size into groups, regardless of location and other
195 factors, allowed us to isolate the effect of fragment size on biological invasion (Hansen et al.,
196 2020). Due to the observed nonlinear relationship, we conducted a piecewise regression (Toms

197 & Lesperance, 2003) and asymptotic regression (Stevens, 1951) to model the nonlinear size
198 effect respectively, and identified two change points derived from these regression models. We
199 assessed the support for the change points by comparing the Akaike information criterion (AIC)
200 of the piecewise model and asymptotic model with the AIC of simple linear model. The mean
201 values of change points were defined as the thresholds to divide mangrove fragments into
202 “small” (below threshold) and “large” (above threshold) (Ordway & Asner, 2020). Because the
203 response variable (i.e., average *S. alterniflora* invasion magnitude) ranged between value of 0
204 and 100%, beta regressions were then applied on both small and large size of mangrove
205 fragments to model the relationship between mangrove size and *S. alterniflora* invasion
206 proportion. For examining the impacts of macroclimatic condition on fragmentation-invasion
207 relationships, we conducted the above statistical analysis for tropical and subtropical
208 mangroves separately.

209 2.4.3. Edge effect on invasion magnitude

210 Mangrove fragments in similar edge proportion were grouped through *K*-means analysis,
211 and a group-level statistical analysis was applied to isolate the effect of fragment edge on
212 biological invasion. We conducted a beta regression model on average invasion magnitude and
213 edge proportion to investigate the edge effect on invasion. Considering the edge proportion
214 may be affected by fragment area, we added the average fragment size into beta regression
215 model as an explanatory variable to account for this interaction effect.

216 To estimate the geographic variation of edge effect on *S. alterniflora* invasion, we further
217 investigated the latitudinal variation of edge effect. For each 0.1° latitudinal band, we regressed
218 invasion magnitude and edge proportion on fragment scale, and defined the edge sensitivity of
219 mangroves to invasion as the slope of the regression models. Preliminary graphical exploration
220 of the relationship between latitude and statistically significant edge sensitivity was conducted
221 to provide details on likely landscape-level patterns. Observed tipping latitude was then

222 identified using piecewise regression model. To investigate potential mechanisms behind the
223 latitudinal variation of edge effect, we used the Normalized Difference Vegetation Index
224 (NDVI) as a proxy of mangrove canopy cover and aboveground biomass (Myneni et al., 1997)
225 to explore the latitudinal trend in mangrove structures.

226 2.4.4. Shape effects on *S. alterniflora* invasion

227 Analysis of variance (ANOVA) and Tukey honestly significant difference (HSD) post-
228 hoc test were conducted to explore the impacts of mangrove fragment shape on *S. alterniflora*
229 invasion. Considering the bias of different sizes of mangrove fragment in same shape, we
230 divided all mangrove fragments into three categories by size through *K*-means algorithm:
231 small-size (< 0.7 ha), medium-size (0.7-24.4 ha) and large-size (> 24.4 ha). Afterwards, we
232 applied a univariate ANOVA on each category to estimate differences among all mangrove
233 shapes, and an HSD post-hoc test to identify the types of shape that related to the least invasion
234 of *S. alterniflora*. Similar analysis was conducted on mangrove fragments which were divided
235 into three groups according to edge area and core area. All statistical analyses were
236 implemented in R version 4.0.0 (R Development Core Team, 2020) using the packages
237 ‘changeoint’ (Killick & Eckley, 2014), ‘segmented’ (Muggeo, 2008) and ‘betareg’ (Cribari-
238 Neto & Zeileis, 2010).

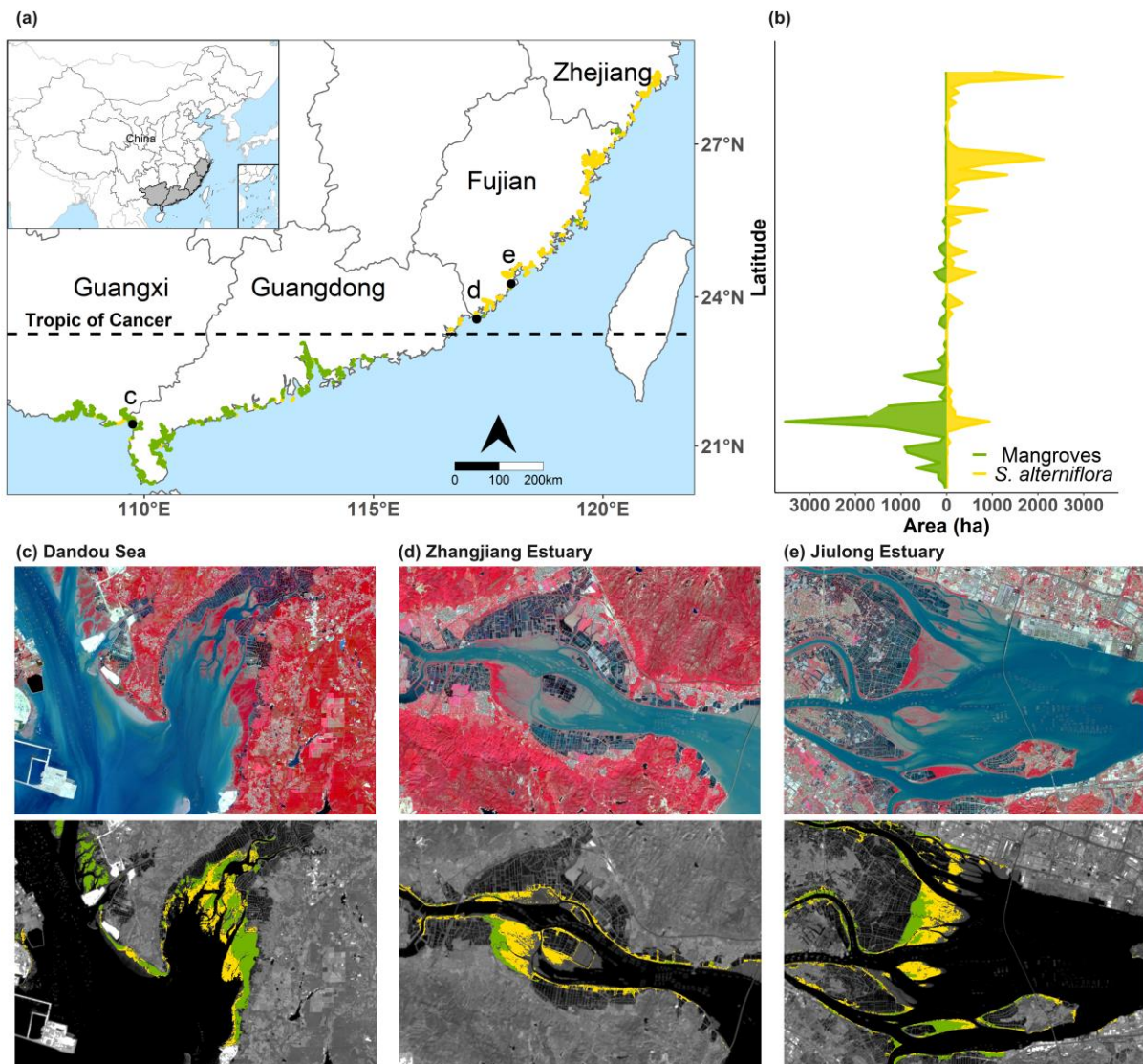
239

240 3. Results

241 3.1. Latitudinal patterns of *S. alterniflora* invasion magnitude

242 According to the distribution of mangroves and *S. alterniflora* derived from remote
243 sensing images, there was 172.46 km² of mangroves and 181.27 km² of *S. alterniflora* in study
244 area (Fig. 2). The variability of the area of mangroves and *S. alterniflora* was observed across
245 the latitudinal gradient (Fig. 2b). As the latitude rises, area of mangrove decreased while that
246 of *S. alterniflora* increased. A significant shift of the mangrove-*S. alterniflora* dominance along

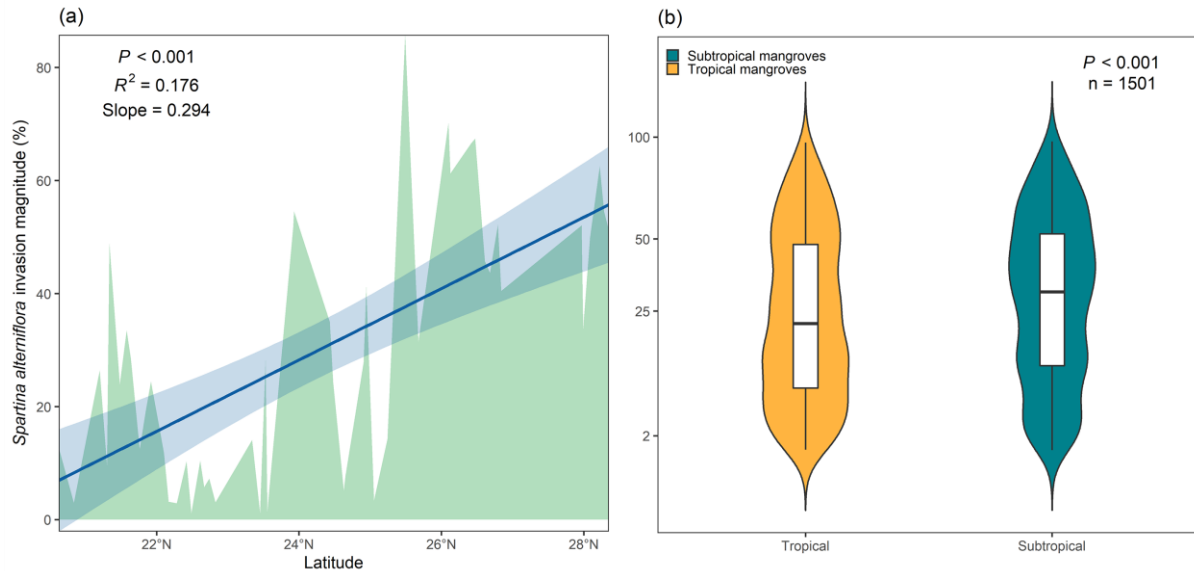
247 latitude were observed near the Tropic of Cancer (23°26'N). In the tropical regions (south of
248 Tropic of Cancer), the total area of mangroves (158.65 km²) was nearly eight times of *S.*
249 *alterniflora* (21.83 km²); while in the subtropical regions, the dominance plant was replaced
250 by *S. alterniflora* (159.44 km²), which was nearly 12 times of mangroves about 13.81 km².



251
252 **Fig. 2.** Spatial distribution of mangroves and *Spartina alterniflora* in 2020. Spatial distribution with 0.1° latitude
253 summaries of mangrove and *S. alterniflora* area are shown as (a) and (b). Three examples of spatial patterns of
254 mangroves and *S. alterniflora* were shown as (c) Dandou Sea, (d) Zhangjiang Estuary, and (e) Jiulong Estuary.
255

256 Major invasion of *S. alterniflora* to mangroves was observed across the study region with
257 a significant increasing trend along latitude from 20°34'N to 28°25'N (Fig. 2 and 3a).
258 Subtropical mangroves had a mean value of 34.0% invaded area by *S. alterniflora*, and the

259 tropical mangroves was about 29.2% (t -test, $p < .001$; Fig. 3b). The distribution of *S.*
260 *alterniflora* invasion suggests that mangroves in subtropical region were more vulnerable in
261 terms of invasion than their tropical counterparts, which was consistent with the spatial
262 distribution of mangrove-*S. alterniflora* dominance.



263
264 **Fig. 3.** Latitudinal variation in the invasion magnitude of *Spartina alterniflora* showing as (a) latitudinal profile
265 and (b) comparison between subtropics and tropic. The observed total amount of invaded mangrove fragments is
266 1501 (751 and 750 in subtropical and tropical regions, respectively). Blue line in (a) represents linear latitudinal
267 trend of invasion magnitude, and blue shaded area is the 95% confidence interval. Green shaded area represents
268 the distribution of invasion magnitude along latitudinal gradient. The boxes in (b) show data within the 25th and
269 75th percentile, black lines show the median values of each group, and violin-shaped area represents distribution
270 of invasion magnitude values. The y axis in (b) was square root-transformed as necessary to comply with
271 parametric assumptions, but show untransformed values.

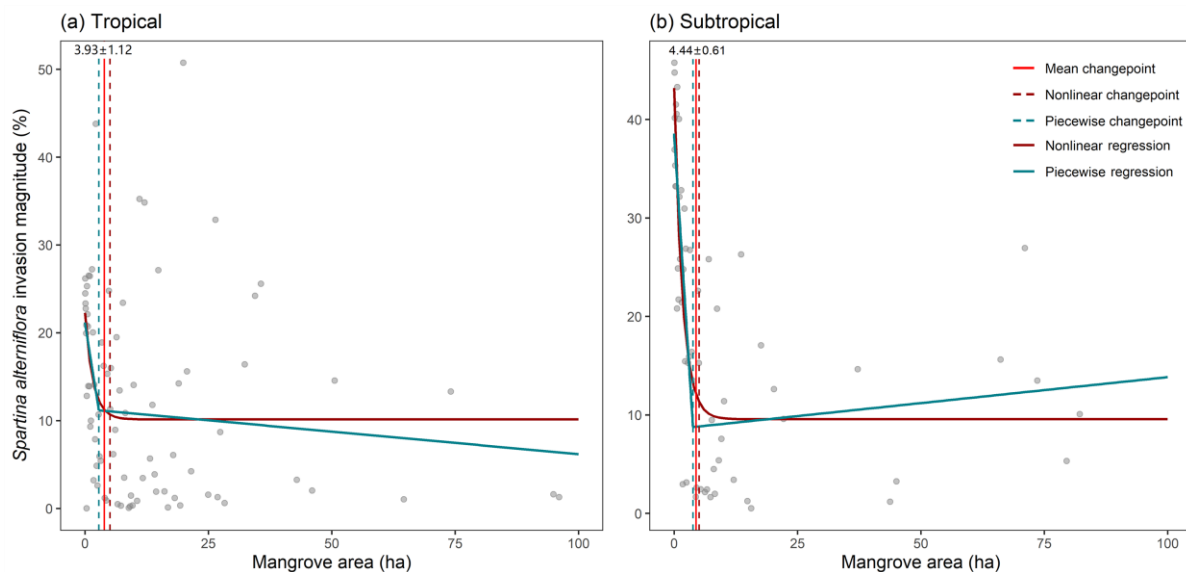
272

273 3.2. Latitudinal variations in mangrove fragmentation and its effects on invasion

274 3.2.1. Fragment size

275 The distribution of average mangrove fragment size follows a decline trend across the
276 latitudinal gradient (Supplemental Fig. S4a), in consistence with the latitudinal trend of total
277 mangrove area. A one-degree increases in latitude resulted in an approximately 0.25 ha
278 decrease of average mangrove fragment size ($R^2 = .101$, $p = .010$). Both piecewise regression
279 and nonlinear asymptotic regression indicated potential nonlinearity in the relationships

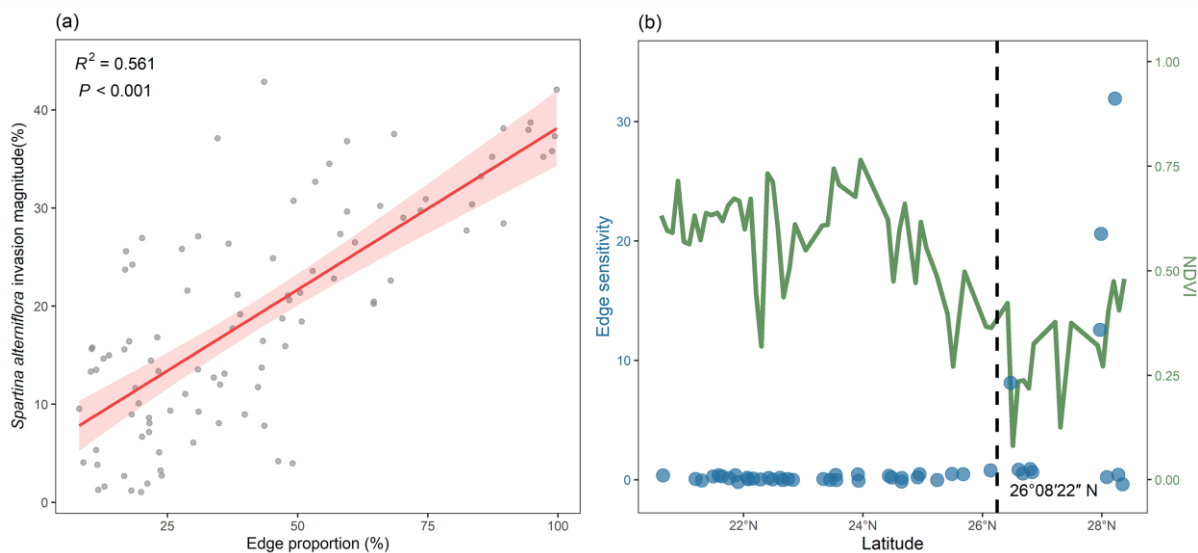
280 between mangrove fragment size and invaded magnitude (supported over linear regression
281 based on lower AIC, $\Delta AIC = 2.5$ and 3.7 for piecewise model and asymptotic model in tropic,
282 and $\Delta AIC = 52.1$ and 55.3 for piecewise model and asymptotic model in subtropics). By
283 combining these two nonlinear models, we found thresholds of mangrove size at the value of
284 3.93 ± 1.12 and 4.44 ± 0.61 ha for tropical and subtropical mangroves, respectively (Fig. 4).
285 Size of mangrove under 4.44 ha in subtropical region was inversely correlated with *S.*
286 *alterniflora* invasion (Pseudo $R^2 = .483$, $p < .001$); however, there is no relationship between
287 the *S. alterniflora* invasion and mangrove size once the mangrove fragment is larger than the
288 threshold value of 4.44 ha (Pseudo $R^2 = .041$, $p = .206$). For tropical mangroves, the relationship
289 between fragment size and *S. alterniflora* invasion magnitude was not statistically significant
290 both in small (Pseudo $R^2 = .002$, $p = .705$) and large mangrove fragments (Pseudo $R^2 = .001$, p
291 $= .834$).



292
293 **Fig. 4.** Effects of mangrove fragment size on invasion magnitude of *Spartina alterniflora* in tropical (a) and
294 subtropical (b) areas. Values between dashed lines are the detected interval of abrupt changes in invasion when
295 size of mangrove fragment increased in certain values. Detailed model parameters are shown in Supplemental
296 Table S3.
297

298 3.2.2. Edge proportion

299 The average edge proportion in each group classified by mangrove edge proportion was
300 related linearly to invasion magnitude of *S. alterniflora* (Fig. 5a), suggesting that mangrove
301 fragments with large proportion of edge belt were particularly sensitive to *S. alterniflora*
302 invasion (Pseudo $R^2 = .561$, $p < .001$). Mangrove fragments with more than 75% of edge area
303 (979 out of 1501 fragments) experienced an average invasion of 34.2%; 263 mangrove
304 fragments with edge proportion of 50-75% showed an average *S. alterniflora* invasion of 26.2%;
305 mangrove forests with 25-50% edge proportion (174 fragments) showed an invasion magnitude
306 of 16.5%; and only 85 mangrove forests with the smallest edge proportion ($< 25\%$ of edge
307 proportion) were exposed to the lowest invasion magnitude of 10.1%. The positive effect of
308 mangrove edge proportion on *S. alterniflora* invasion magnitude was modified by an
309 interaction between edge proportion and size ($\Delta AIC = 1.2$ comparing the full linear model with
310 or without interaction), with edge effect will be minimized when the mangrove fragment size
311 increases (slope = -0.001 , $p = .036$, Supplemental Table S4).



312
313 **Fig. 5.** Edge effects of invasion magnitude. (a) Relationship between edge proportion and *Spartina alterniflora*
314 invasion magnitude. The shaded area indicates the 95% confidence interval of regression. (b) Edge sensitivity
315 (regression slope of edge effect) and NDVI of mangroves along latitude (average value of mangrove forests in
316 each 0.1° latitudinal band). The vertical dashed line shows the latitudinal change point (26°08'22" N).

317

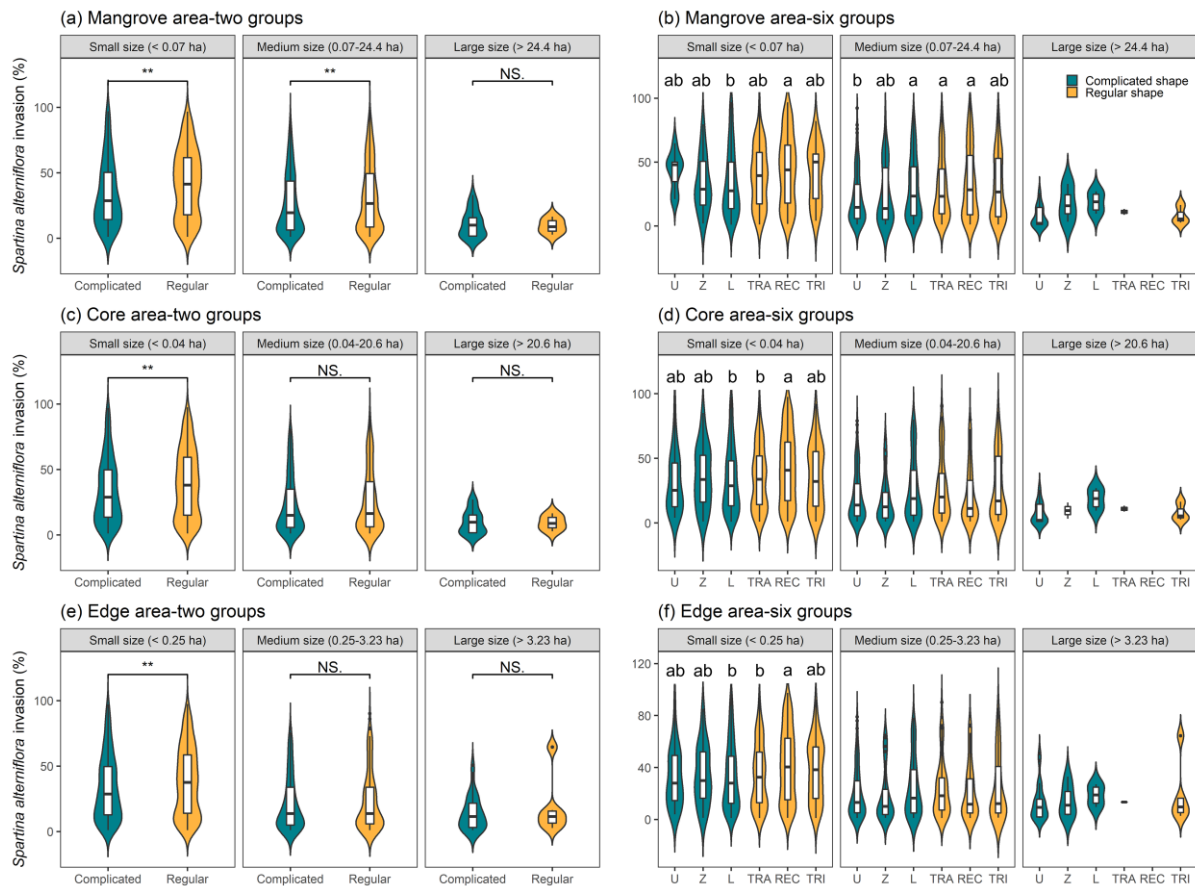
318 As the edge proportion of mangrove fragments increases with latitude, the increased edge
319 effect implies that subtropical mangroves are particularly sensitive to *S. alterniflora* invasion
320 (Supplemental Fig. S4b). Observing the edge sensitivity of mangroves across latitude through
321 a piecewise model ($\Delta AIC = 5.2$ comparing with the linear model), we detected a latitudinal
322 change point at the location of $26^{\circ}08'N$ (95% Confidence Interval (CI) = $25^{\circ}16'$ to $27^{\circ}22'$; Fig
323 5b), adjacent to the northern limit of natural mangrove distribution in China ($27^{\circ}20'N$). The
324 latitudinal fluctuation of mangrove NDVI provides a direct estimation of changes in mangrove
325 canopy cover and biomass (Fig. 5b), which explained the phenomenon of abrupt shift of edge
326 effect on invasion across the latitudinal tipping point. It exhibited a latitudinal heterogeneity in
327 the north part of this change point, suggesting that the resistance of planted mangroves to *S.*
328 *alterniflora* invasion was more susceptible to change of edges.

329 3.2.3. Fragment shape

330 Different to former two metrics, latitudinal trend of mangrove fragment shape was not
331 significant (Supplemental Fig. S4c). Comparing the *S. alterniflora* invasion in different shapes
332 of mangroves, we found that invasion magnitude varied significantly in different-shaped
333 fragments ($p < .05$; Fig. 6a). Regarding the small (< 0.7 ha) and medium size (0.7-24.4 ha) of
334 mangroves, fragments with regular shapes of triangle, trapezoid and rectangle appeared to have
335 an average invasion magnitude of $31.78\% \pm 1.82\%$ (95% CI), which was substantially larger
336 than mangrove fragment with complicated U, L and Z-shapes by $26.20\% \pm 1.81\%$ (95% CI).
337 But the effect of different shapes in large-sized mangroves (> 24.4 ha) was not observed (p
338 = .681; Supplemental Table S5).

339 In addition, we conducted similar analysis on different-shaped mangroves with
340 considering different edge and core area of each mangrove fragment (Fig. 6c, e). In terms of
341 invasive magnitude, we observed a significant difference between regular and complicated
342 shapes only in small-size groups with edge area < 0.25 ha and core area < 0.04 ha. This finding

343 indicates the impact of mangrove fragment shapes on *S. alterniflora* invasion existed in the
 344 case of fragmented mangrove communities with small-sized core area and edge area.



345 **Fig. 6.** Comparing *Spartina alterniflora* invasion by size (a, b), core area (c, d) and edge area (e, f) of mangrove
 346 fragments. Values of *S. alterniflora* invasion area were indicated by violin plot regarding different shapes of
 347 mangrove fragment. Welch's *t*-test was used to estimate differences between complicated and regular-shaped
 348 mangroves. One-way ANOVA was conducted to evaluate the differences of invasion among all six shapes. Boxes
 349 in the middle of each dataset show the interquartile ranges, and solid lines in the box indicate the median value of
 350 such dataset. Letters above violin plot bars denote significant difference among shapes resulting from multiple
 351 comparison analysis. Different letters indicate significant differences ($p < .05$) among mangrove fragment shapes.
 352 Individual statistical values for each subplot are presented in Supplemental Table S5. Series with double asterisk
 353 (**) means the correlation analysis of $p < .01$, and NS. stands for non-significant at the level of $p > .05$.
 354 Abbreviation of shapes are list as TRA-trapezoid, REC-rectangle, TRI-triangle.

355
 356
 357 The largest invasive magnitude was observed in the rectangle-shaped (regular shape)
 358 mangrove fragments, which was higher than trapezoid-shaped (regular shape) mangroves by
 359 $7.33\% \pm 6.87\%$ (95% CI) and L-shaped (complicated shape) mangrove fragments by $9.80\% \pm$
 360 8.21% (95% CI; Fig. 6b; Supplemental Table S5). The small size of L-shaped mangrove

361 fragments had the most stable structure to minimize *S. alterniflora* invasion, which signifies
362 the L-shaped mangrove fragments have a high level of resistance in invasion challenges of *S.*
363 *alterniflora*.

364

365 **4. Discussion**

366 Spatial detection of the mangrove-*S. alterniflora* ecotone is of great value to understand
367 dynamics of biological invasion in coastal wetlands. This study, to our knowledge, is the first
368 to examine relationships between mangrove fragmentation and its invaded magnitude at a
369 landscape scale. We found that fragmentation of mangrove forests would promote the invasive
370 magnitude of *S. alterniflora*, and this relationship varies between latitudes and climate zones.
371 Our findings highlight the value of large scale and biogeographic perspective on mangrove
372 fragmentation and biological invasion, with the goal of informing policy and ecosystem
373 management in the future.

374 **4.1. Latitudinal trends in mangroves and *S. alterniflora***

375 Our study indicates that the invasion magnitude of *S. alterniflora* on native mangroves
376 increased with increasing latitude, suggesting the mangrove community may be more
377 susceptible to invasion at higher than at lower latitudes. This response is consistent with
378 biogeographical patterns of their climatic niche, and agrees with previous study which
379 indicated the aboveground biomass of *S. alterniflora* increases with latitude in Southern China
380 (Liu et al., 2020). In low latitudes, climate conditions are suitable for survival and dispersal of
381 freeze-sensitive mangroves, enhancing their competition on habitat niche with invasive salt
382 marsh (Cavanaugh et al., 2019). Conversely, the expansion of mangrove forests in subtropical
383 and temperate regions is limited by its climate conditions, which in turn facilitate the invasion
384 of freeze-tolerant salt marshes (Osland et al., 2017). Another possible explanation of this
385 latitudinal pattern may be that the species richness of mangrove communities may decrease as

386 the latitude rises, weakening the biotic resistance to invaders (Beaury et al., 2020; Guo et al.,
387 2020; Wu et al., 2018).

388 **4.2. Fragmentation-invasion relationships in mangrove-salt marsh ecotone**

389 The negative nonlinearity in size effect implies that small mangrove fragments are
390 particularly sensitive to *S. alterniflora* invasion as compared to large mangrove blocks. While
391 the size effect is not significant in tropic, the constrain effect of size on relationship between
392 edge proportion and invaded magnitude is significant on whole ecotone. Our findings reveal
393 that large mangrove fragments exhibit stronger resistance to salt marsh invasion. This is
394 consistent with previous studies indicating that large and highly connected patches could
395 enhance dispersal ability and system's robustness to stochastic perturbations (Wintle et al.,
396 2019). Although the loss of small mangrove fragments may seem less concerning than large-
397 scale invasion, their interconnectedness with adjacent habitats allows them to provide
398 substantial ecosystem services as stepping stones to link local systems (Curnick et al., 2019).
399 In addition, the invasion of small-sized mangroves would create barriers to species that depend
400 on mangroves, erodes local coastal resilience and pushes mangrove ecosystems toward
401 collapse. Therefore, protecting small mangrove fragments and preventing further mangrove
402 fragments split into several smaller ones becomes the critical task in maintaining resilience in
403 coastal ecosystems.

404 Our study highlights that the edge proportion of mangrove fragments was related with the
405 incidence of plant invasions. Ecological effects arising from edges between mangrove and non-
406 mangrove habitat change biophysical environments for adjacent habitats, generating the local
407 conditions in which invasive species seem to thrive, such as canopy gaps and areas with high
408 light levels (Li et al., 2014). Previous field experiment-based study also revealed that mangrove
409 edge creates an open and low canopy structure in local community, which reduces herbivore
410 activity but increases light availability, resulting in erosion of resistance of mangrove forests

411 to *S. alterniflora* invasion (Zhang et al., 2018). We found that edge sensitivity of mangroves to
412 invasion dramatically shifts at the location of 26°08'N (95% CI = 25°16' to 27°22'N), which
413 is near with the northern limit (27°20'N) of natural mangroves distribution (Chen et al., 2017),
414 and is consistent with latitudinal variation of mangrove NDVI. This consistent geographic
415 change point reveals that small fragmented mangroves with open canopy and planted
416 mangroves are more susceptible to invasions.

417 Comparisons between multiple mangrove shapes suggests that the shape of mangrove
418 fragments has significant impacts on salt marsh invasion, particularly in small and medium-
419 sized mangrove fragments. Since there is no significant latitudinal trend in the shape of
420 mangrove fragments, it is inferred that the shape effects on invasion may occur in most regions.
421 Previous theory has noted that an ecologically optimum fragment shape tends to has a large
422 core with some curvilinear boundaries and narrow lobes (Forman, 1995; Moser et al., 2002),
423 but have yet to point specific shapes which have higher resistance to invasion. Here we report
424 that mangrove fragments with regular shapes were more susceptible to *S. alterniflora* invasion,
425 and rectangle was identified as the shape undergoing more severe salt marsh invasion and lower
426 resistance. This can be explained by the resistance of mangrove fragments to external
427 perturbations from nature environmental, is usually controlled by core area and interaction with
428 adjacent habitats, both of which are determined by the shape of source fragments (Orrock et
429 al., 2011). For testing the explanatory of core area on shape effect, we conducted an analysis
430 of covariance (ANCOVA), which could control variable of total area in shapes that related with
431 low invasion, and found that trapezoidal and L-shaped mangrove fragments have larger
432 proportion of core area than that of rectangle (Supplemental Fig. S5). Additionally, mangrove
433 fragments with trapezoid or L shape tend to have a large perimeter and size, thus these types
434 of mangroves have a large biotic and abiotic flow with adjacent habitats and higher dispersal
435 ability (Lester et al., 2007). As a result, fragment shapes with sufficient core area and

436 curvilinear boundaries, such as L shape and trapezoid, exhibit stronger resistance to biological
437 invasion (Rastandeh & Pedersen Zari, 2018).

438 **4.3. Management implications for mangrove forests**

439 Several global conservation policy mechanisms have included mangroves in their targets,
440 such as the Mangroves for the Future and Sustainable Development Goals 14.5 and Target 11
441 in Aichi Targets (Friess et al., 2019). Regional governments have also taken actions into
442 mangrove conservation. For example, Chinese government has established twenty-eight
443 Protection Areas, which has protected 67% of the mangrove forests in China (Wang et al.,
444 2020). The key way to achieve these goals is mangroves planting. However, results have shown
445 large-scale replant planning did not lead to expected long-term mangrove area increases (Lee
446 et al., 2019). In China, about half of the replanted mangroves have failed to restored, which is
447 partly due to the invasion of *S. alterniflora* into suitable mangrove niche (Chen et al., 2009).
448 Management and conservation of mangroves are therefore required for alleviating biological
449 invasion stresses, which can be achieved by controlling landscape patterns of mangrove
450 fragments in local communities according to our findings. The edge and shape sensitivity of
451 mangroves to *S. alterniflora* invasion underpins effective guidance in rehabilitating and
452 protecting existed mangrove fragments to improve their resistance to invasions. Moreover,
453 preventing extant mangrove blocks divide into multiple smaller fragments should be a
454 management priority wherever possible, especially for the subtropical mangroves due to their
455 critical vulnerability to exotic species invasion. Paying more attentions to the size and edge
456 proportion of replanted mangrove forests and prevent further mangrove fragmentation are
457 crucial to mangrove conservation, especially in the regions beyond the geographic range limit
458 of natural mangroves distribution.

459 Optimum fragment shape also needs to be considered in mangroves rehabilitation and
460 management. The L- and trapezoid-shaped mangrove are recommended in this study as suitable

461 fragment shapes to resist the invasion of alien species. Current mangrove restoration mainly
462 focuses on natural environment, which neglects spatial structure and pattern of mangrove
463 forests. Spatial characters, such as fragment size, edge proportion and fragment shape, should
464 be incorporated to generate more effective restoration approach to enhance the resistance and
465 resilience of mangroves and regional biosecurity.

466 **4.4. Limitations**

467 Although we presented observational evidences on the relationships between mangrove
468 fragmentation and *S. alterniflora* invasion magnitude, there is still uncertainties associated with
469 them as they were developed under some limitations. First, fragmentation metrics (fragment
470 size, edge proportion and fragment shape) were calculated from raster dataset, which can be
471 biased by its spatial resolution even if we use the highest resolution available remote sensing
472 data (i.e., Sentinel-2 at 10-m resolution). Another limitation is except for the spatial distribution
473 of the tidal flats, salinity gradient, soil texture, and tidal range may also affect the extent of
474 potential mangrove habitat. These environmental factors can hardly be included in our analysis
475 due to the lack of high-resolution data at the landscape scale.

476

477 **5. Conclusions**

478 By combining remote-sensing detection and landscape analysis, we demonstrate that
479 fragmentation of mangrove forests increased the invaded magnitude by *S. alterniflora*, and this
480 effect varies with latitudes and climate zones. We found that mangrove fragments with small
481 size, large edge proportion and regular boundary shape are particularly sensitive to plant
482 invasion. This has important conservation implications because mangroves are facing threats
483 from both fragmentation and biological invasion globally. Our results indicate that the
484 fragmentation-invasion relationships are ubiquitous throughout the whole mangrove-salt marsh
485 ecotone, but intensified in subtropical regions, the inappropriate climatic area for freeze-

486 sensitive mangroves. These findings suggest an urgent need for management strategy to
487 mitigate fragmentation of mangrove forests, particularly in subtropical mangroves, and
488 highlight that optimizing landscape pattern should be considered as an effective strategy for
489 addressing the ongoing biological invasions, and can be used to navigate native species
490 management actions for making management efforts more informed and effective.

491

492 **Declarations**

493 **Acknowledgements**

494 This research was supported by the National Natural Science Foundation of China (NSFC)
495 Grant No.41701205 and Fundamental Research Funds for the Central Universities
496 No.20720190089.

497 **Conflicts of Interest/Competing interests**

498 Authors report no conflicts of interest.

499 **Availability of data and material**

500 All datasets used in this study are publicly available. The Sentinel-2 L2A Surface Reflectance
501 (https://developers.google.com/earthengine/datasets/catalog/COPERNICUS_S2_SR); The
502 Global Mangrove Watch dataset (<https://data.unep-wcmc.org/datasets/45>); the Global Tidal
503 Flats dataset (<https://www.intertidal.app/>).

504 **Code availability**

505 The code is available from <https://github.com/GIS-ZhangZhen/Edge-sensitivity-of-mangroves>.

506 **CRedit authorship contribution statement**

507 **ZZ:** Conceptualization; Methodology; Software; Formal analysis; Writing - Original Draft;
508 Visualization

509 **JL:** Methodology; Formal analysis; Visualization

510 **Yi L:** Conceptualization; Writing - Review & Editing; Resources; Funding acquisition; Project
511 administration

512 **WL:** Conceptualization; Formal analysis; Writing-Review & Editing

513 **YC:** Conceptualization; Formal analysis; Writing-Review & Editing

514 **YZ:** Conceptualization; Writing - Review & Editing

515 **Yangfan L:** Conceptualization; Resources

516

517 **References**

518 Aguirre-Acosta, N., Kowaljow, E., & Aguilar, R. (2014). Reproductive performance of the
519 invasive tree *Ligustrum lucidum* in a subtropical dry forest: does habitat fragmentation boost
520 or limit invasion? *Biological Invasions*, *16*, 1397–1410.

521 Alofs, K.M. & Jackson, D.A. (2014). Meta-analysis suggests biotic resistance in freshwater
522 environments is driven by consumption rather than competition. *Ecology*, *95*, 3259–3270.

523 Beaury, E.M., Finn, J.T., Corbin, J.D., Barr, V. & Bradley, B.A. (2020). Biotic resistance to
524 invasion is ubiquitous across ecosystems of the United States. *Ecology Letters*, *23*, 476–482.

525 Bellard, C., Cassey, P., Blackburn, T.M. (2016). Alien species as a driver of recent extinctions.
526 *Biology Letters*, *12*, 20150623.

527 Biswas, S.R., Biswas, P.L., Limon, S.H., Yan, E.R., Xu, M.S., Khan, M.S.I. (2018). Plant
528 invasion in mangrove forests worldwide. *Forest Ecology and Management*, *429*, 480–492.

529 Bradley, B. A., Blumenthal, D. M., Early, R., Grosholz, E. D., Lawler, J. J., Miller, L. P., Sorte,
530 C.J.B., D’Antonio, C.M., Diez, J.M., Dukes, J.S., Ibanez, I., Olden, J.D. (2012). Global
531 change, global trade, and the next wave of plant invasions. *Frontiers in Ecology and the*
532 *Environment*, *10*, 20–28.

533 Bryan-Brown, D.N., Connolly, R.M., Richards, D.R., Adame, F., Friess, D.A. & Brown, C.J.
534 (2020). Global trends in mangrove forest fragmentation. *Scientific Reports*, *10*, 7117.

- 535 Bunting, P., Rosenqvist, A., Lucas, R., Rebelo, L.M., Hilarides, L., Thomas, N., Hardy, A.,
536 Itoh, T., Shimada, M., Finlayson, C. (2018). The global mangrove watch—a new 2010 global
537 baseline of mangrove extent. *Remote Sensing*, *10*, 1669.
- 538 Cavanaugh, K.C., Dangremond, E.M., Doughty, C.L., Williams, A.P., Parker, J.D., Hayes,
539 M.A., Rodriguez, W., Feller, I.C. (2019). Climate-driven regime shifts in a mangrove-salt
540 marsh ecotone over the past 250 years. *Proceedings of the National Academy of Sciences of*
541 *the United States of America*, *116*, 21602–21608.
- 542 Chaplin-Kramer, R., Ramler, I., Sharp, R., Haddad, N.M., Gerber, J.S., West, P.C., Mandle, L.,
543 Engstrom, P., Baccini, A., Sim, S., Mueller, C., King, H. (2015). Degradation in carbon
544 stocks near tropical forest edges. *Nature Communications*, *6*, 10158.
- 545 Chen, Y., Li, Y., Cai, T., Thompson, C., Li, Y. (2016). A comparison of biohydrodynamic
546 interaction within mangrove and saltmarsh boundaries. *Earth Surface Processes and*
547 *Landforms*, *41*, 1967–1979.
- 548 Chen, B., Xiao, X., Li, X., Pan, L., Doughty, R., Ma, J., Dong, J., Qin, Y., Zhao, B., Wu, Z.,
549 Sun, R., Lan, G., Xie, G., Clinton, N., Giri, C. (2017). A mangrove forest map of China in
550 2015: Analysis of time series Landsat 7/8 and Sentinel-1A imagery in Google Earth Engine
551 cloud computing platform. *ISPRS Journal of Photogrammetry and Remote Sensing*, *131*,
552 104–120.
- 553 Chen, L., Wang, W., Zhang, Y. & Lin, G. (2009). Recent progresses in mangrove conservation,
554 restoration and research in China. *Journal of Plant Ecology*, *2*, 45–54.
- 555 Cornelissen, B., Neumann, P. & Schweiger, O. (2019). Global warming promotes biological
556 invasion of a honey bee pest. *Global Change Biology*, *25*, 3642–3655.
- 557 Cribari-Neto, F. & Zeileis, A. (2010). Beta regression in R. *Journal of Statistical Software*, *34*,
558 1–24.

- 559 Curnick, D.J., Pettorelli, N., Amir, A.A., Balke, T., Barbier, E.B., Crooks, S., Dahouh-Guebas,
560 F., Duncan, C., Endsor, C., Friess, D.A., Quarto, A., Zimmer, M., Lee, S.Y. (2019). The value
561 of small mangrove patches. *Science*, *363*, 239.
- 562 Dawson, W., Burslem, D.F.R.P., & Hulme, P.E. (2015). Consistent Effects of Disturbance and
563 Forest Edges on the Invasion of a Continental Rain Forest by Alien Plants. *Biotropica*, *47*,
564 27–37.
- 565 Donato, D.C., Kauffman, J.B., Murdiyarto, D., Kurnianto, S., Stidham, M. & Kanninen, M.
566 (2011). Mangroves among the most carbon-rich forests in the tropics. *Nature Geoscience*, *4*,
567 293–297.
- 568 Forman, R.T.T. (1995). Some general principles of landscape and regional ecology. *Landscape*
569 *Ecology*, *10*, 133–142.
- 570 Friess, D.A., Rogers, K., Lovelock, C.E., Krauss, K.W., Hamilton, S.E., Lee, S.Y., Lucas, R.,
571 Primavera, J., Rajkaran, A., Shi, S. (2019). The State of the World's Mangrove Forests: Past,
572 Present, and Future. *Annual Review of Environment and Resources*, *44*, 89–115.
- 573 Gorelick, N., Hancher, M., Dixon, M., Ilyushchenko, S., Thau, D. & Moore, R. (2017). Google
574 Earth Engine: Planetary-scale geospatial analysis for everyone. *Remote Sensing of*
575 *Environment*, *202*, 18–27.
- 576 Guo, Q., Cade, B.S., Dawson, W., Essl, F., Kreft, H., Pergl, J., van Kleunen, M., Weigelt, P.,
577 Winter, M., Pyšek, P. (2020). Latitudinal patterns of alien plant invasions. *Journal of*
578 *Biogeography*, *00*, 1–10.
- 579 Haddad, N.M., Brudvig, L.A., Clobert, J., Davies, K.F., Gonzalez, A., Holt, R.D., Lovejoy,
580 T.E., Sexton, J.O., Austin, M.P., Collins, C.D., Cook, W.M., Damschen, E.L., Ewers, R.M.,
581 Foster, B.L., Jenkins, C.N., King, A.J., Laurance, W.F., Levey, D.J., Margules, C.R.,
582 Melbourne, B.A., Nicholls, A.O., Orrock, J.L., Song, D.X., Townshend, J.R. (2015). Habitat
583 fragmentation and its lasting impact on Earth's ecosystems. *Science Advances*, *1*, e1500052.

584 Hansen, M.C., Wang, L., Song, X.P., Tyukavina, A., Turubanova, S., Potapov, P.V. & Stehman,
585 S.V. (2020). The fate of tropical forest fragments. *Science Advances*, *6*, eaax8574.

586 Kelleway, J. J., Cavanaugh, K., Rogers, K., Feller, I. C., Ens, E., Doughty, C., & Saintilan, N.
587 (2017). Review of the ecosystem service implications of mangrove encroachment into salt
588 marshes. *Global Change Biology*, *23*, 3967–3983.

589 Killick, R. & Eckley, I.A. (2014). Changepoint: An R package for changepoint analysis.
590 *Journal of Statistical Software*, *58*,1–19.

591 Lee, S.Y., Hamilton, S., Barbier, E.B., Primavera, J. & Lewis, R.R. (2019). Better restoration
592 policies are needed to conserve mangrove ecosystems. *Nature Ecology & Evolution*, *3*, 870–
593 872.

594 Lester, S.E., Ruttenberg, B.I., Gaines, S.D. & Kinlan, B.P. (2007). The relationship between
595 dispersal ability and geographic range size. *Ecology Letters*, *10*, 745–758.

596 Li, Z., Wang, W., & Zhang, Y. (2014). Recruitment and herbivory affect spread of invasive
597 *Spartina alterniflora* in China. *Ecology*, *95*, 1972–1980.

598 Lin, J. (1991). Divergence measures based on the Shannon entropy. *IEEE Transactions on*
599 *Information Theory*, *37*, 145–151.

600 Liu, M., Mao, D., Wang, Z., Li, L., Man, W., Jia, M., Ren, C., Zhang, Y. (2018). Rapid invasion
601 of *Spartina alterniflora* in the coastal zone of mainland China: New observations from
602 Landsat OLI images. *Remote Sensing*, *10*, 1933.

603 Liu, W., Chen, X., Strong, D.R., Pennings, S.C., Kirwan, M.L., Chen, X. & Zhang, Y. (2020).
604 Climate and geographic adaptation drive latitudinal clines in biomass of a widespread
605 saltmarsh plant in its native and introduced ranges. *Limnology and Oceanography*, *65*, 1399–
606 1409.

- 607 Liu, W., Maung-Douglass, K., Strong, D.R., Pennings, S.C. & Zhang, Y. (2016). Geographical
608 variation in vegetative growth and sexual reproduction of the invasive *Spartina alterniflora*
609 in China. *Journal of Ecology*, *104*, 173–181.
- 610 Malavasi, M., Carboni, M., Cutini, M., Carranza, M.L. & Acosta, A.T.R. (2014). Landscape
611 fragmentation, land-use legacy and propagule pressure promote plant invasion on coastal
612 dunes: a patch-based approach. *Landscape Ecology*, *29*, 1541–1550.
- 613 Mendes, C.P., Ribeiro, M.C. & Galetti, M. (2016). Patch size, shape and edge distance
614 influence seed predation on a palm species in the Atlantic forest. *Ecography*, *39*, 465–475.
- 615 Meng, W., Feagin, R.A., Innocenti, R.A., Hu, B., He, M. & Li, H. (2020). Invasion and
616 ecological effects of exotic smooth cordgrass *Spartina alterniflora* in China. *Ecological*
617 *Engineering*, *143*, 105670.
- 618 Moser, D., Zechmeister, H.G., Plutzer, C., Sauberer, N., Wrba, T. & Grabherr, G. (2002).
619 Landscape patch shape complexity as an effective measure for plant species richness in rural
620 landscapes. *Landscape Ecology*, *17*, 657–669.
- 621 Muggeo, V.M. (2008). Segmented: An R package to fit regression models with broken-line
622 relationships. *R News*, *8*, 20–25.
- 623 Murray, N.J., Phinn, S.R., DeWitt, M., Ferrari, R., Johnston, R., Lyons, M.B., Clinton, N.,
624 Thau, D., Fuller, R.A. (2019). The global distribution and trajectory of tidal flats. *Nature*,
625 *565*, 222–225.
- 626 Myneni, R.B., Keeling, C.D., Tucker, C.J., Asrar, G. & Nemani, R.R. (1997). Increased plant
627 growth in the northern high latitudes from 1981 to 1991. *Nature*, *386*, 698–702.
- 628 Oehri, J., Schmid, B., Schaepman-Strub, G. & Niklaus, P.A. (2017). Biodiversity promotes
629 primary productivity and growing season lengthening at the landscape scale. *Proceedings of*
630 *the National Academy of Sciences of the United States of America*, *114*, 10160–10165.

- 631 Ordway, E.M. & Asner, G.P. (2020). Carbon declines along tropical forest edges correspond
632 to heterogeneous effects on canopy structure and function. *Proceedings of the National*
633 *Academy of Sciences of the United States of America*, 117, 7863–7870.
- 634 Orrock, J.L., Gregory, R.C., Danielson, B.J., Coyle, D.R. (2011). Large-scale experimental
635 landscapes reveal distinctive effects of patch shape and connectivity on arthropod
636 communities. *Landscape Ecology*, 26, 1361–1372.
- 637 Osland, M.J., Day, R.H., Hall, C.T., Brumfield, M.D., Dugas, J.L. & Jones, W.R. (2017).
638 Mangrove expansion and contraction at a poleward range limit: climate extremes and land-
639 ocean temperature gradients. *Ecology*, 98, 125–137.
- 640 Osland, M.J., Enwright, N.M., Day, R.H., Gabler, C.A., Stagg, C.L. & Grace, J.B. (2016).
641 Beyond just sea-level rise: Considering macroclimatic drivers within coastal wetland
642 vulnerability assessments to climate change. *Global Change Biology*, 22, 1–11.
- 643 R Development Core Team (2020). R: A language and environment for statistical computing.
644 Vienna, Austria: R Foundation for Statistical Computing. Retrieved from [https://www.R-](https://www.R-project.org/)
645 [project.org/](https://www.R-project.org/).
- 646 Rastandeh, A. & Pedersen Zari, M. (2018). A spatial analysis of land cover patterns and its
647 implications for urban avifauna persistence under climate change. *Landscape Ecology*, 33,
648 455–474.
- 649 Richards, D.R. & Friess, D.A. (2016). Rates and drivers of mangrove deforestation in Southeast
650 Asia, 2000-2012. *Proceedings of the National Academy of Sciences of the United States of*
651 *America*, 113, 344–349.
- 652 Slingsby, J.A., Merow, C., Aiello-Lammens, M., Allsopp, N., Hall, S., Kilroy Mollmann, H.,
653 Turner, R., Wilson, A.M., Silander, J.A. (2017). Intensifying postfire weather and biological
654 invasion drive species loss in a Mediterranean-type biodiversity hotspot. *Proceedings of the*
655 *National Academy of Sciences of the United States of America*, 114, 4697–4702.

- 656 Stevens, W.L. (1951). Asymptotic regression. *Biometrics*, 7, 247–267.
- 657 Stotz, G.C., Gianoli, E. & Cahill, J.F. (2016). Spatial pattern of invasion and the evolutionary
658 responses of native plant species. *Evolutionary Applications*, 9, 939–951.
- 659 Toms, J.D. & Lesperance, M.L. (2003). Piecewise regression: a tool for identifying ecological
660 thresholds. *Ecology*, 84, 2034–2041.
- 661 van Kleunen, M., Bossdorf, O. & Dawson, W. (2018). The ecology and evolution of alien
662 plants. *Annual Review of Ecology, Evolution, and Systematics*, 49, 25–47.
- 663 Vaz, A.S., Alcaraz-Segura, D., Campos, J.C., Vicente, J.R. & Honrado, J.P. (2018). Managing
664 plant invasions through the lens of remote sensing: A review of progress and the way forward.
665 *Science of the Total Environment*, 642, 1328–1339.
- 666 Vilà, M. & Ibáñez, I. (2011). Plant invasions in the landscape. *Landscape Ecology*, 26, 461–
667 472.
- 668 Waddell, E.H., Banin, L.F., Fleiss, S., Hill, J.K., Hughes, M., Jelling, A., Yeong, K.L., Ola,
669 B.B., Sailim, A.B., Tangah, J., Chapman, D.S. (2020). Land-use change and propagule
670 pressure promote plant invasions in tropical rainforest remnants. *Landscape Ecology*, 35,
671 1891–1906.
- 672 Wang, W., Fu, H., Lee, S.Y., Fan, H. & Wang, M. (2020). Can strict protection stop the decline
673 of mangrove ecosystems in china? From rapid destruction to rampant degradation. *Forests*,
674 11, 55.
- 675 Wintle, B.A., Kujala, H., Whitehead, A., Cameron, A., Veloz, S., Kukkala, A., Moilanen, A.,
676 Gordon, A., Lentini, P.E., Cadenhead, N.C.R., Bekessy, S.A. (2019). Global synthesis of
677 conservation studies reveals the importance of small habitat patches for biodiversity.
678 *Proceedings of the National Academy of Sciences of the United States of America*, 116, 909–
679 914.

- 680 Worthington, T.A., Andradi-Brown, D.A., Bhargava, R., Buelow, C., Bunting, P., Duncan, C.,
681 Fatoyinbo, L., Friess, D.A., Goldberg, L., Hilarides, L., Lagomasino, D., Landis, E., Longley-
682 Wood, K., Lovelock, C.E., Murray, N.J., Narayan, S., Rosenqvist, A., Sievers, M., Simard,
683 M., Thomas, N., van Eijk, P., Zganjar, C., Spalding, M. (2020). Harnessing big data to
684 support the conservation and rehabilitation of mangrove forests globally. *One Earth*, 2, 429–
685 443.
- 686 Wu, Y., Ricklefs, R.E., Huang, Z., Zan, Q. & Yu, S. (2018). Winter temperature structures
687 mangrove species distributions and assemblage composition in China. *Global Ecology and*
688 *Biogeography*, 27, 1492–1506.
- 689 Zhang, Y., Huang, G., Wang, W., Chen, L. & Lin, G. (2012). Interactions between mangroves
690 and exotic *Spartina* in an anthropogenically disturbed estuary in southern China. *Ecology*, 93,
691 588–597.
- 692 Zhang, Y., Meng, H., Wang, Y. & He, Q. (2018). Herbivory enhances the resistance of
693 mangrove forest to cordgrass invasion. *Ecology*, 99, 1382–1390.